

AD-A282 020



June 16, 1994

Reprint

VARIABILITY OF SOLAR MESOGRANULATION

PE 61102F
PR 2311
TA G3
WU 27

G.W. Simon, L.J. November*, L.W. Acton**, S.H. Ferguson**,
R.A. Shine**, T.D. Tarbell**, A.M. Title**, K.P. Topka**,
H. Zirin#

Phillips Lab/GPSS
29 Randolph Road
Hanscom AFB, MA 01731-3010

PL-TR-94-2166

*National Solar Observatory, Sunspot NM 88349 **Lockheed Palo Alto
Research Laboratory, 3251 Hanover Street, Palo Alto CA 94304 #California Institute
of Technology, Pasadena CA 91125

Reprinted from Adv. Space Res. Vol. 8, No. 7 pp (7)69-(7)72 1988

Approved for public release; distribution unlimited

DTIC
SELECTED
JUN 29 1994
S B D

From white-light photographs of solar granulation obtained with the SOUP instrument on Space Shuttle Flight STS-19 we have measured the motions of granules using local correlation tracking techniques. The granules are organized into larger-scale structures (mesogranular and supergranular) which exhibit outflow from upwellings, convergence into sinks, as well as significant vorticity. Magnetic fields follow these same flow patterns. We describe these velocity structures, and suggest that their effect on magnetic field structures may be important to the solar flare buildup process.

94-19786



94 6 28 130

14. SUBJECT TERMS Granulation, Mesogranulation, Supergranulation, magneto-convection, velocity field, magnetic fields			15. NUMBER OF PAGES 4
			16. PRICE CODE
17. SECURITY CLASSIFICATION OF REPORT UNCLASSIFIED	18. SECURITY CLASSIFICATION OF THIS PAGE UNCLASSIFIED	19. SECURITY CLASSIFICATION OF ABSTRACT UNCLASSIFIED	20. LIMITATION OF ABSTRACT SAR

NSN 7540-01-280-5500

DTIC QUALITY INSPECTED

Standard Form 298 (Rev. 2-89)
Prescribed by ANSI Std. Z39-18
298-102

VARIABILITY OF SOLAR MESOGRANULATION

G. W. Simon,* L. J. November,** L. W. Acton,***
S. H. Ferguson,*** R. A. Shine,*** T. D. Tarbell,***
A. M. Title,*** K. P. Topka*** and H. Zirin†

*Air Force Geophysics Laboratory, Sunspot, NM 88349, U.S.A.

**National Solar Observatory, Sunspot, NM 88349, U.S.A.

***Lockheed Palo Alto Research Laboratory, 3251 Hanover St., Palo Alto,
CA 94304, U.S.A.

†California Institute of Technology, Pasadena, CA 91125, U.S.A.

ABSTRACT

From white-light photographs of solar granulation obtained with the SOUP instrument on Space Shuttle Flight STS-19 we have measured the motions of granules using local correlation tracking techniques. The granules are organized into larger-scale structures (mesogranular and supergranular) which exhibit outflow from upwellings, convergence into sinks, as well as significant vorticity. Magnetic fields follow these same flow patterns. We describe these velocity structures, and suggest that their effect on magnetic field structures may be important to the solar flare buildup process.

OBSERVATIONS

The SOUP (Solar Optical Universal Polarimeter) experiment /1/ built by the Lockheed Palo Alto Research Laboratory obtained a 27.5 min movie of solar granulation during orbit 110 (19.10–19.38 UT 5 Aug 1985) of the Spacelab 2 (STS-19) Space Shuttle mission. Because the images are free of distortion by the earth's atmosphere, it is possible to detect very small motions (less than 5 km) of solar intensity features, using the method of local correlation tracking /2,3/. These data show that solar granules move like test particles ("corks") on top of larger-scale longer-lived flow patterns in the solar atmosphere. These structures are predominantly mesogranular size (4"–12"), although a few have supergranular (20"–40") scales (1" = one arcsec = 720 km).

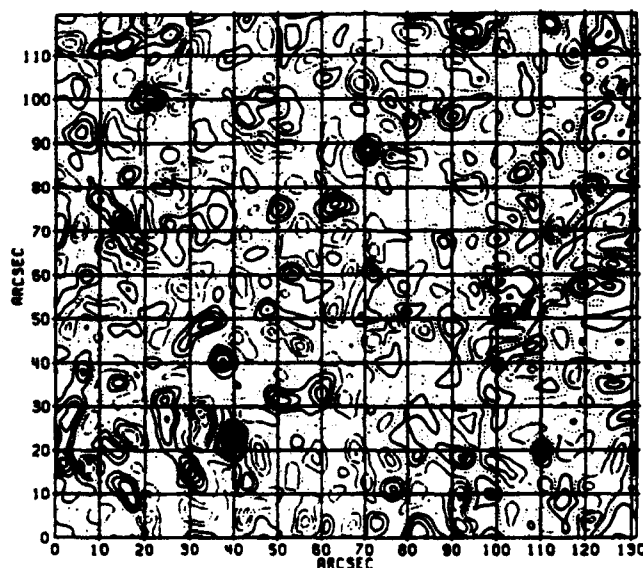


Fig. 1. Contour plot of the divergence field. Solid contours are sources, dashed ones are sinks.

ANALYSIS

If one computes the divergence Δ and the vertical component of the vorticity ω from the observed horizontal flow vector \mathbf{v} at each point in the area of observation:

$$\Delta = \frac{\partial v_x}{\partial x} + \frac{\partial v_y}{\partial y} \quad \omega_z = \frac{\partial v_y}{\partial x} - \frac{\partial v_x}{\partial y}, \quad (1)$$

one finds that the sun is covered by mesogranular-sized sources and sinks (where Δ has positive and negative extrema, respectively) and centers of twist (extrema of ω_z). In Figure 1 we show a contour diagram of Δ over a $131'' \times 119''$ portion of the SOUP image area. There are approximately one source and one sink in an area $10'' \times 10''$. In Figure 2 we show twelve particularly good examples of positive and negative divergence extracted from Figure 1.

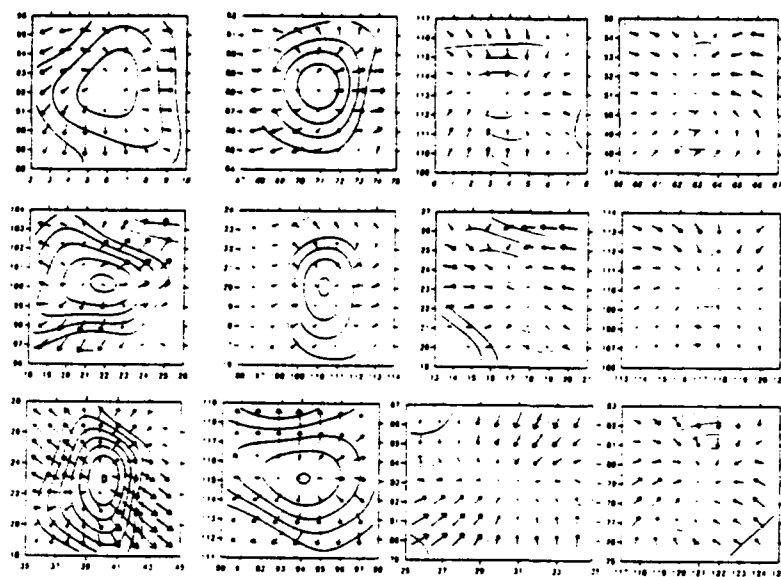


Fig. 2. Twelve examples of diverging and converging flows. The six left-hand images are sources; the six right-hand ones are sinks. Numbers along the abscissa and ordinate of each small figure correspond to the same numbers in Fig. 1.

The vorticity map has a very similar appearance, and contains about the same number of clockwise and counterclockwise vortices. We show in Figure 3 six cases of each.

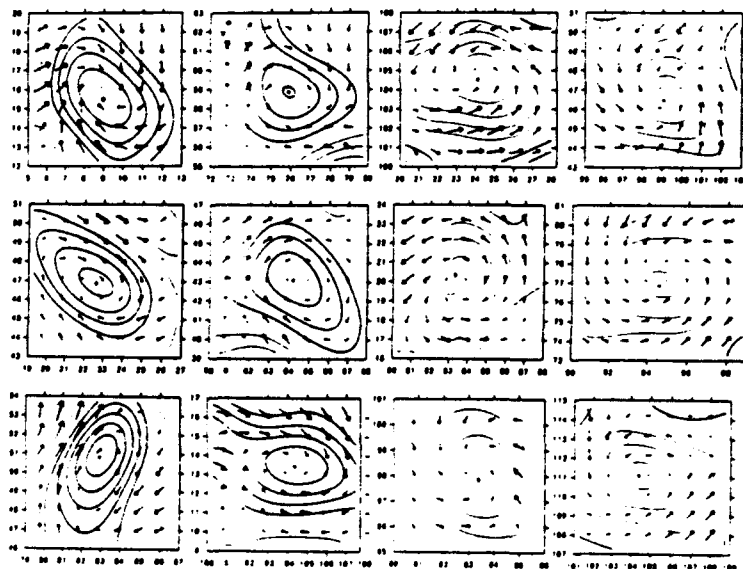


Fig. 3. Twelve examples of vertical vorticity. Six clockwise flows are shown on the left, and six counterclockwise on the right.

Typical values for the local maxima of Δ and ω_z are 0.5 to 1.5 h^{-1} . An interesting observation is that the maxima and minima of vorticity only rarely occur at the same loci as the maxima or minima of divergence. This disagrees with one's intuitive expectation that the flow would probably follow a vortical path as it is sucked into a sink.

We have determined the size distribution of these structures and the separation distance between adjacent sources. These are shown in Figure 4. The half-size (radius) of a feature is defined as the

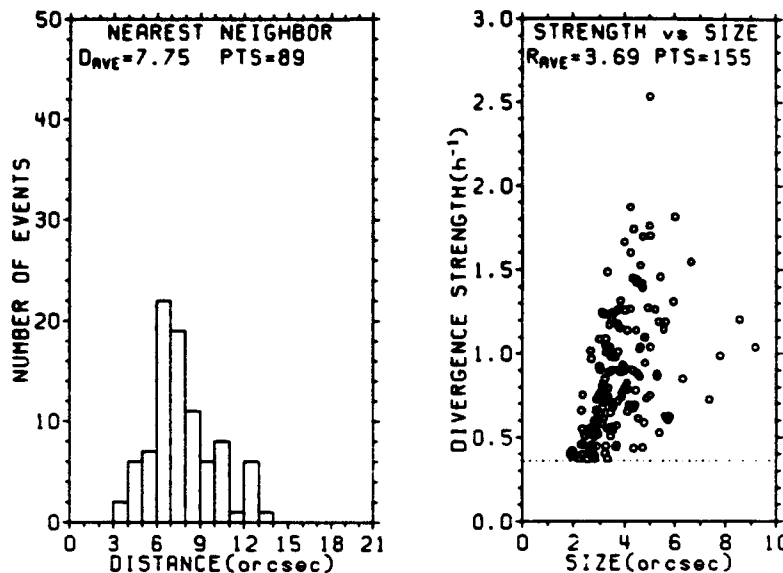


Fig. 4. (Right) Strength vs. size of divergence maxima. No strengths below the noise level of 0.36 h^{-1} are shown. (Left) Distance to nearest neighbor of each maximum shown in Fig. 4 (right). Points within $10''$ of the area boundary were excluded from the analysis, as were points with strength less than 0.54 h^{-1} .

distance from its center (where the divergence has its maximum, or "strength") to the point where the divergence drops to zero. The measured radii are shown in Figure 4 (right), as a function of strength. The average diameter (size) of such a feature is $7''$ to $8''$, with most structures ranging from $4''$ to $12''$ in size. Figure 4 (left) is a histogram of the distance from each feature to its nearest neighbor, and has a mean value of about $8''$. The range of separations is $4''$ to $15''$, much smaller than the distances one would expect if the field consisted of supergranules ($20''$ to $40''$).

Despite the rarity of supergranular-sized structures in these velocity data, these larger features, though mainly hidden by the smaller mesogranules, do exist. This can be seen when we consider the motions of corks subjected to the measured velocity field. In Figure 5 we show the positions of such corks in a $65'' \times 65''$ area of the SOUP image 1, 2, 4, 8, 16, and 32 h after the corks start from a uniform distribution. It can be seen (by comparing Figure 5 with Figure 1) that the corks move first to mesogranular boundaries, then develop into a larger (supergranular) structure, and finally concentrate and disappear into sinks. One should note a basic assumption we have made in producing this cork time-series; namely, that the velocity field, obtained during a 27.5 min observing sequence, remains constant for the entire length of the cork series.

CONCLUSIONS

By correlating these flows with simultaneous observations of the solar magnetic field we have found /4/ that magnetic flux elements move in patterns which are in almost perfect agreement with those of the granular corks: Magnetic features are expelled from the centers of mesogranules, moving first to the mesogranular boundaries and ending up at the boundaries (network) of the larger supergranules. Contrary to the corks, which fall into sinks, the magnetic elements apparently prefer to remain primarily as a network pattern.

These observations have important implications for the buildup of magnetic activity on the sun. Since the structure of the sun's surface magnetic field closely mimics that of velocity corks, the motions of granular corks should help one to determine where magnetic fields will pile up and undergo stress. In addition, since the observed vorticities are large enough to twist a magnetic flux tube by a full 360° in less than three hours, it should become possible to pinpoint loci of magnetic mixing and twisting, and thus to increase one's ability to predict the occurrence of solar flares, coronal heating, and mass ejections.

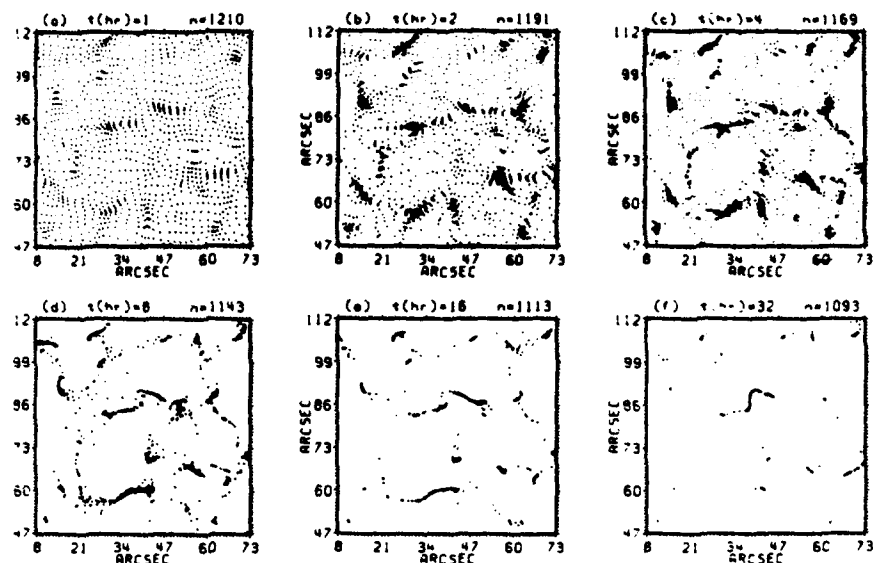


Fig. 5. Cork motions in a 65" x 65" section of the SOUP field of Fig. 1.

REFERENCES

1. Title, A., Tarbell, T., Simon, G. and the SOUP Team, *Adv. Space Res.* 6, 253 (1986)
2. November, L., *Appl. Optics* 25, 392 (1986)
3. November, L. and Simon, G., *Ap. J.* 333, in press (1 October) (1988)
4. Simon, G., Title, A., Topka, K., Tarbell, T., Shine, R., Ferguson, S., Zirin, H. and the SOUP Team, *Ap. J.* 327, 964 (1988)

Accession For	
NTIS GRA&I	<input checked="" type="checkbox"/>
DTIC TAB	<input type="checkbox"/>
Unannounced	<input type="checkbox"/>
Justification	
By	
Distribution	
Availability Codes	
Dist	Avail and/or Special
A-1	20